Articles

Crystal Structure of the Rac1−RhoGDI Complex Involved in NADPH Oxidase Activation[†,‡]

S. Grizot,[§] J. Fauré,[||,⊥] F. Fieschi,[§] P. V. Vignais,[||] M.-C. Dagher,*[,||] and E. Pebay-Peyroula*[,§]

Institut de Biologie Structurale, CEA-CNRS-UJF, UMR 5075, 41 Rue Jules Horowitz, 38027 Grenoble Cedex 1, France, and Laboratoire BBSI/CEA-CNRS-UJF, UMR 5092/Département de Biologie Moléculaire et Structurale/CEA Grenoble, 17 Rue des Martyrs, 38054 Grenoble Cedex 9, France

Received February 9, 2001; Revised Manuscript Received May 15, 2001

ABSTRACT: A heterodimer of prenylated Rac1 and Rho GDP dissociation inhibitor was purified and found to be competent in NADPH oxidase activation. Small angle neutron scattering experiments confirmed a 1:1 stoichiometry. The crystal structure of the Rac1−RhoGDI complex was determined at 2.7 Å resolution. In this complex in which Rac1 is bound to GDP, the switch I region of Rac1 is in the GDP conformation whereas the switch II region resembles that of a GTP-bound GTPase. Two types of interaction between RhoGTPases and RhoGDI were investigated. The lipid−protein interaction between the geranylgeranyl moiety of Rac1 and RhoGDI resulted in numerous structural changes in the core of RhoGDI. The interactions between Rac1 and RhoGDI occur through hydrogen bonds which involve a number of residues of Rac1, namely, $Tyr64_{Rac}$, $Arg66_{Rac}$, $His103_{Rac}$, and $His104_{Rac}$, conserved within the Rho family and localized in the switch II region or in its close neighborhood. Moreover, in the switch II region of Rac1, hydrophobic interactions involving $Leu67_{Rac}$ and $Leu70_{Rac}$ contribute to the stability of the Rac1−RhoGDI complex. Inhibition of the GDP−GTP exchange in Rac1 upon binding to RhoGDI partly results from interaction of $Thr35_{Rac}$ with $Asp45_{GDI}$. In the Rac1−RhoGDI complex, the accessibility of the effector loops of Rac1 probably accounts for the ability of the Rac1−RhoGDI complex to activate the NADPH oxidase.

The small G protein, Rac, a member of the Rho family, plays essential roles in a large variety of cellular processes, such as cell growth, the regulation of the actin cytoskeleton (*1*), and the inflammatory response, via the activation of the stress-activated protein kinases p38 and c-Jun kinase (*2*). Rac has also a key role in the assembly and activation of phagocyte NADPH oxidase (*3*). Rac cycles between an inactive GDP-bound state and an active GTP-bound state. This cycle is tightly regulated by guanine−nucleotide exchange factors (GEFs)[1] that catalyze the GDP−GTP exchange reaction and by GTPase-activating proteins (GAPs) that enhance the intrinsic GTPase activity of the small G proteins (*4*). Rac undergoes a posttranslational modification that allows its localization to the plasma membrane. It consists of the covalent binding of a geranylgeranyl group to the cysteine residue of the C-terminal CAAX motif via a thioether linkage, a reaction that is catalyzed by a geranylgeranyl transferase. The last three amino acids are then released, and the C-terminal cysteine residue is carboxymethylated. Three isoforms of Rac have been reported in humans, namely, Rac1, which is ubiquitously expressed, Rac2, which is predominantly present in the cells of the myeloid lineage (*5*), and Rac3, which was recently cloned from a breast cancer cell line (*6*).

In resting cells, most of the Rho-related proteins are located in the cytosol, associated with a GDP dissociation inhibitor protein, RhoGDI (*7*), which is ubiquitously expressed. Another isoform, called LyGDI (also termed D4-GDI or RhoGDI2), is only present in the hematopoietic tissues (*8*, *9*). A third isoform, RhoGDIγ, with an N-terminal extension of 20 amino acids, was shown to be preferentially expressed in brain and pancreas (*10*). RhoGDI was first isolated as an inhibitor protein for the GDP−GTP exchange reaction on RhoB (*11*). RhoGDI inhibits the release of GDP from the active site of the RhoGTPases. It can also associate with the GTP-bound form of Rho proteins, and then it inhibits the intrinsic and GAP-catalyzed GTPase activity of

[†] This work was supported by the PCV-CNRS program, the Emergence/Region-Rhone-Alpes program, the Direction Générale des Forces et de la Prospective, the Fondation pour la Recherche Médicale, and the Association pour la Recherche sur le Cancer.

[‡] The coordinates and the structure factors have been deposited in the Protein Data Bank with ID code 1hh4.

* Corresponding authors.

[§] Institut de Biologie Structurale, CEA-CNRS-UJF, UMR 5075.

[||] Laboratoire BBSI/CEA-CNRS-UJF, UMR 5092/Département de Biologie Moléculaire et Structurale/CEA Grenoble.

[⊥] Present address: Laboratoire de Biochimie, Université Sciences II, 30 quai E. Ansermet, 1211 Geneva-4, Switzerland.

[1] Abbreviations: GEF, guanine−nucleotide exchange factor; GAP, GTPase-activating protein; GDI, guanine−nucleotide dissociation inhibitor; ERM, ezrin, radixin, and moesin; rmsd, root mean square deviation; CRIB, Cdc42/Rac interaction binding.

10.1021/bi010288k CCC: $20.00
Published on Web 08/03/2001

these proteins (*12*). In fact, RhoGDI can bind in vitro to the Rho proteins in both of their conformational states with almost the same affinity (*13*). Another property of RhoGDI is its ability to extract Rho-related proteins from the membrane, thereby controlling the balance between an inactive cytosolic pool of GDP-bound Rho proteins associated with RhoGDI and the active membrane-bound pool. Although the effect of RhoGDI on RhoGTPases is well documented, the regulation of the interaction between the two proteins is less well understood. Phosphoinositides have been shown to partially open the RhoA−RhoGDI complex, allowing the RhoA protein to exchange GDP for GTP (*14*). It has also been suggested that proteins of the ERM family act as dissociation factors for the RhoA−RhoGDI complex (*15*). Regulation may also occur by proteolysis of RhoGDI. Indeed, the isoform LyGDI can be cleaved by caspases during inflammatory or apoptotic processes (*16*−*18*).

We report here the three-dimensional crystal structure of the complex between Rac1 and RhoGDI at 2.7 Å resolution as well as a biochemical study on the effect of the Rac1−RhoGDI complex on the NADPH oxidase activation. Comparison of this structure with that of Cdc42−RhoGDI (*19*) and Rac2−LyGDI (*20*) highlights the specificity of RhoGDI for the Rho proteins among the large family of small GTPases. In the Rac1−RhoGDI complex, RhoGDI stabilizes a GTP-like conformation of the switch II region of Rac1 while amino acids critical for NADPH oxidase activation remain accessible. The physiological implications of these structural aspects are discussed.

EXPERIMENTAL PROCEDURES

Purification of Rac1−RhoGDI and Small Angle Neutron Scattering Experiments. Sf9 cells were coinfected with two baculoviruses encoding Rac1 and His−RhoGDI. The expression and purification of the complex were identical to the protocol described for RhoA−RhoGDI (*14*). The nickel affinity chromatography column was followed by a Superdex 75 gel filtration column (Pharmacia) equilibrated in 10 mM Tris-HCl, pH 7.5, 5 mM $MgCl_2$, and 150 mM NaCl. The complex was then concentrated on Centricon 10 (Amicon). The RhoGDI homodimer that coeluted with the Rac1−RhoGDI heterodimer was removed by chromatography on a MonoQ anion-exchange column (Pharmacia) after a 2-fold dilution in 10 mM Tris-HCl, pH 7.5, and 5 mM $MgCl_2$. The Rac1−RhoGDI heterodimer was eluted by 100 mM NaCl, well separated from the RhoGDI dimer that was eluted by 300 mM NaCl. SANS experiments were performed on beamline D11 at ILL (Grenoble) as described (*21*). The Rac1−RhoGDI heterodimer was concentrated to 10 mg/mL. The protein concentration was derived from amino acid analysis.

Assay of NADPH Oxidase Activity. NADPH oxidase activating potency of the Rac−RhoGDI heterodimer was determined in a semirecombinant cell-free system containing 6 μg of membrane protein, 200 pmol of p67phox N-ter(1−240), 20 pmol of p47phox, 10−100 pmol of Rac1 bound to RhoGDI, and an optimal amount of arachidonic acid (10−20 nmol) in a final volume of 200 μL of PBS. As a control, Rac1 was preloaded with GTP-γ-S by incubation with 10 mM EDTA and 10 μM GTP-γ-S for 10 min at 25 °C followed by addition of $MgCl_2$ to 20 mM. After 10 min at 25 °C, the superoxide dismutase inhibitable cytochrome *c* reduction was followed at 550 nm in the presence of 100 μM cytochrome *c* and 250 μM NADPH.

Table 1: Statistics for X-ray Structure Determination

data collection statistics	
resolution range (Å)	30−2.7
total reflections	50106
unique reflections	21165
redundancy	2.36 (2.28)[e]
completeness (%)	84.7 (80.6)[e]
I/σ	13.0 (2.1)[e]
R_{sym}[a] (%)	6.2 (43.4)[e]
refinement statistics	
resolution range (Å)	20−2.7
R_{cryst}[b] (%)	25.6
R_{free}[c] (%)	28.0
no. of non-hydrogen atoms[d]	
protein	5813
ligand	98
solvent	30
rms deviations	
bonds (Å)	0.009
angles (deg)	1.59
average *B*-factor (Å^2)	57.1

[a] $R_{sym} = \sum\sum|I_j - \langle I\rangle|/\sum\langle I\rangle$. [b] Crystallographic *R*-factor = $100[\sum(||F_o| - |F_c||)/\sum|F_o|]$ where F_o and F_c are respectively the observed and calculated structure factor amplitudes. [c] R_{free} is the crystallographic *R*-factor calculated for a subset of randomly selected reflections (5%) and not used in the refinement process. [d] A restrained noncrystallographic symmetry was applied on the main chain atoms of the two complexes during the refinement. [e] Quantities calculated in the highest resolution shell are indicated in parentheses (2.76−2.70 Å).

Crystallization of the Rac1−RhoGDI Complex. Crystals were grown at 20 °C by vapor diffusion in hanging drops by mixing equal volumes of protein solution (8−10 mg/mL) and reservoir solution (30% PEG 4000, 100 mM sodium citrate, pH 5.6, 5 mM $MgCl_2$, and 200 mM ammonium acetate). The crystals are small needles with a typical size of 30 × 30 × 100 μm^3. They belong to the orthorhombic space group $P2_12_12$ with unit cell dimensions $a = 154.7$ Å, $b = 88.7$ Å, and $c = 62.6$ Å and contain two complexes in the asymmetric unit related by a 2-fold axis parallel to the *b* axis as seen from the self-Patterson function.

Data Collection and Structure Determination. A data set at 100 K was collected on a flash-frozen crystal at 2.7 Å on beam line ID14-EH4 at ESRF (Grenoble). Data were processed and scaled by DENZO and SCALEPACK (*22*). Statistics are given in Table 1. A first partial model was obtained using the molecular replacement method with Rac1 and RhoGDI (PDB accession codes 1MH1 and 1RHO) as search models. The program AmoRe (*23*) showed clearly two positions for Rac1 but none for RhoGDI. Initial phases calculated with the two Rac1 molecules did not allow the reconstruction of RhoGDI. Molecular replacement done with a low-resolution structure of the RhoA−RhoGDI complex did not improve the phasing (*24*). RhoGDI was finally positioned using the structure of Cdc42−RhoGDI (*19*). Initial rigid body refinement gave an *R*-factor of 37.7% on the structure factor amplitudes.

Structure Refinement. The structure was built and refined through alternating cycles using the programs O (*25*) and CNS (*26*). One GDP molecule and one Mg^{2+} per complex were clearly visible. Residues absent in the search model could be built in the density during the refinement. The final

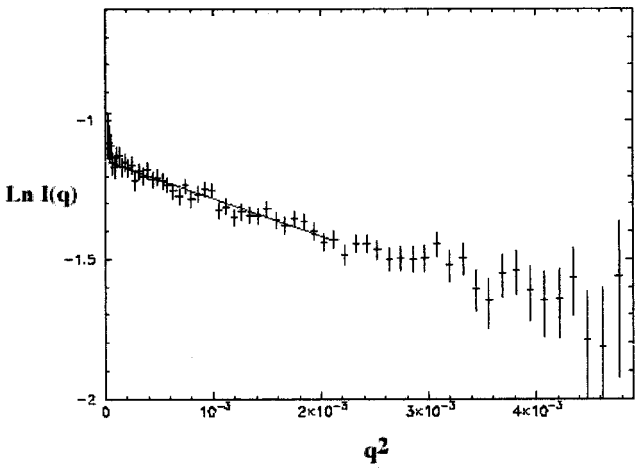

FIGURE 1: SANS experiment on the Rac1−RhoGDI heterodimer. The plot represents ln $I(q)$, where $I(q)$ is the normalized scattered intensity, as a function of q^2 (Å^{-2}), where $q = 4\pi \sin \theta/\lambda$, 2θ is the scattering angle, and λ is the wavelength. The radius of gyration, R_g, is obtained from a linear fit at low q values ($R_g q < 1$, Guinier approximation).

model includes two Rac1−RhoGDI heterodimers in the asymmetric unit. Each complex comprises residues 1−189 of Rac1 and its geranylgeranyl modification, a GDP molecule, a Mg^{2+}, residues 9−201 of RhoGDI, and 30 water molecules. The N-terminus until amino acid 20 for RhoGDI and loop 58−66 of RhoGDI are disordered in one complex of the asymmetric unit. We used a restrained noncrystallographic symmetry on the main chain atoms between the two complexes of the asymmetric unit during all the refinement process, and we refined only two *B*-factors per residue. The mean *B*-factor over the complex (57.1 Å^2) is comparable to the temperature factor derived from the Wilson plot (58 Å^2). Residues 183−189 of Rac1, the N-terminus, and a few loops of RhoGDI exhibit *B*-factors exceeding 100 Å^2. Water molecules were added during the refinement process when electron density was visible in both the $2F_o - F_c$ map contoured at 1σ and in the $F_o - F_c$ map contoured at 3σ. The model was controlled with a simulated annealing combined omit map calculated over the whole structure. The final model has an R_{cryst} of 25.6% and an R_{free} of 28.0%. All the residues are within the allowed region of the Ramachandran plot, among which 78% lay in the most favorable region. Figures were prepared with MOLSCRIPT (*27*) and Raster3D (*28*).

RESULTS

Biochemical and Biophysical Characterization of the Rac1−RhoGDI Complex. The Rac1−RhoGDI complex eluted as a dimer from the gel filtration column. An excess of RhoGDI homodimer that coeluted in the gel filtration fractions was eliminated by anion-exchange chromatography. Small angle neutron scattering (SANS) experiments confirmed a 1:1 stoichiometry in solution. The Guinier plot (Figure 1) shows that the solution is monodisperse with a molecular mass of 44.4 kDa for the scattering species, consistent with the theoretical mass of the Rac1−RhoGDI complex, which is 48.7 kDa. From the slope of the Guinier plot, a radius of gyration of 28 Å was deduced. As shown in Figure 2, this complex was able to activate the NADPH oxidase in a cell-free system as efficiently as isolated Rac1

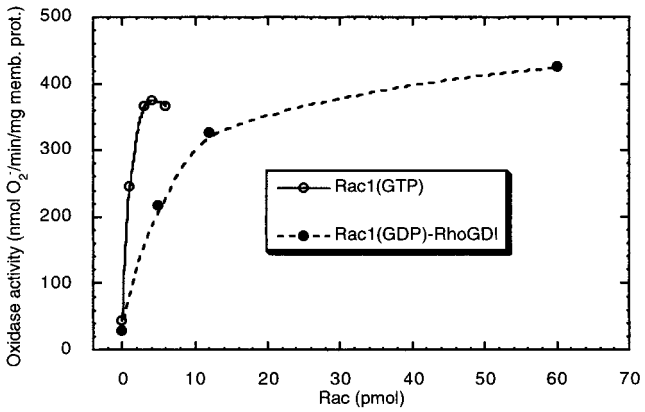

FIGURE 2: NADPH oxidase activating potency of the Rac1−RhoGDI complex. An aliquot of the complex used for crystallization was tested for its NADPH oxidase activating potency in a cell-free system as described in Experimental Procedures (full circles). The activation curve with Rac1(GTP) is shown in parallel (open circles).

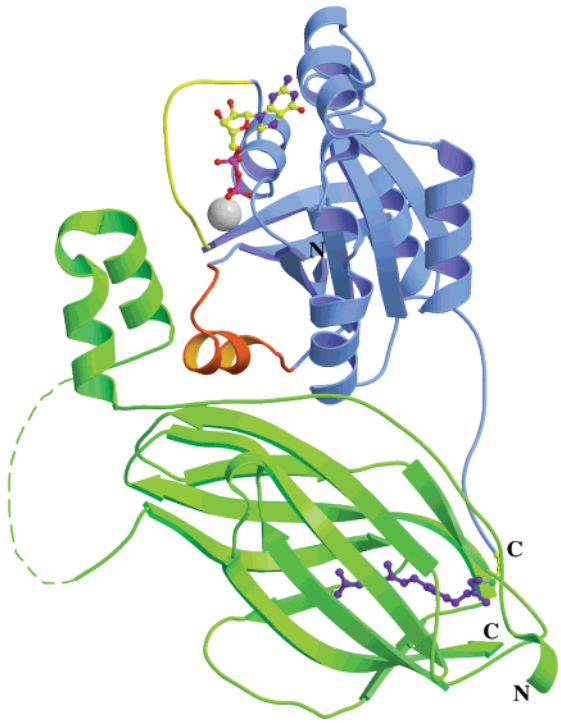

FIGURE 3: Ribbon representation of the Rac1−RhoGDI complex. Rac1 is depicted in blue and RhoGDI in green. The switch I and II regions are highlighted in yellow and red, respectively. The GDP molecule and geranylgeranyl group are represented in ball and sticks. Mg^{2+} is shown in gray. Loop $(58-66)_{GDI}$ (dashed line) is not visible in the crystallographic structure.

protein preloaded with GTP-γ-S, except that a 10-fold higher amount of complexed Rac was required compared to the isolated protein.

Analysis of the Structure of the Rac1−RhoGDI Complex. The overall structures of Rac1 and RhoGDI in the Rac1−RhoGDI complex are similar to the structures of the isolated proteins. Figure 3 shows a ribbon representation of the Rac1−RhoGDI heterodimer. The figure highlights the switch I and II regions of Rac1 involved in nucleotide binding and the geranylgeranyl group bound to the C-terminus of Rac1. In the Rac1−RhoGDI complex, Rac1 binds one guanine nucleotide and one Mg^{2+}. From the electron density map, this nucleotide is assigned to GDP. The structure of Rac1

bound to RhoGDI is similar to the structure of RhoA(GDP) (*29*) with a rmsd of 0.90 Å. On the basis of the structure of the Ras protein, two regions of the small GTPases, switch I (residues 28−40) and switch II (residues 59−74), have been found to undergo conformational changes during the GDP−GTP exchange reaction. In the Rac1−RhoGDI complex, the switch I region of Rac1 is in a GDP-like conformation. Comparison of the switch II region of the Rac1(GDP)−RhoGDI complex with that of Rac1(GMPPNP) (*30*) and that of RhoA(GDP) (*29*) shows rmsd values of 0.45 and 1.23 Å, respectively (rmsd are calculated for the Cα atoms of switch II residues). This led us to conclude that, in the Rac1−RhoGDI structure, the conformation of switch II of Rac1 is close to that of a GTP-bound Rho protein. This conclusion is in agreement with the rmsd value of 0.43 Å calculated for the switch II region of RhoA(GTP-γ-S) (*31*). Since some residues of switch II of Rac1 interact with RhoGDI, RhoGDI might constrain and stabilize a GTP-like conformation of the switch II region. However, as discussed (*19*), the difference between the GTP-bound conformation and the GDP-bound conformation of switch II is less pronounced than in the case of Ras proteins. The insert region spanning residues 122−137 is a unique feature of the Rho-related GTPases. From deletion experiments, it has been postulated that the insert of Cdc42 might be involved in the interaction with RhoGDI (*32*). The Rac1−RhoGDI structure shows that the insert region of Rac1 does not interact with RhoGDI and that the above data may be explained by long-distance conformational changes. The C-terminal end of Rac1 encompassing residues 180−189 is poorly defined with high *B*-factors, but the 20 carbon atom chain characteristic of the geranylgeranyl group of Rac1 is visible in the electron density map in the hydrophobic pocket of the immunoglobulin-like domain of RhoGDI.

Several studies in solution had shown that the N-terminal region of RhoGDI up to residue 60 is very flexible and disordered although it is required for the inhibition of GDP−GTP exchange (*33*, *34*). Within the Rac1−RhoGDI complex, the N-terminal region of RhoGDI which extends from residue 9 to residue 25 is not well defined and does not display any secondary structure. Residues 34−55 of RhoGDI fold into two antiparallel α-helices that pack against the switch I region of Rac1, therefore constraining its conformation (Figure 3). The core structure of RhoGDI spanning residues 70−200 adopts an immunoglobulin-like fold which comprises nine β-strands, labeled βA to βI, organized in two antiparallel sheets such as in the truncated isolated protein. By comparison with the structure of RhoGDI (*34*), the rmsd calculated for the Cα atoms of residues 70−200 is 1.2 Å. A long loop (residues 58−66) joining this C-terminal domain to the structured N-terminal domain is poorly defined in the electron density map.

The Isoprenyl-Binding Domain. Previous structural studies on Rho-like proteins have been restricted to proteins devoid of the isoprenyl moiety. In more recent crystallographic studies, the GTPases in the Cdc42−RhoGDI complex (*19*) and Rac2−LyGDI complex (*20*) were isoprenylated. In the Rac1−RhoGDI complex examined in the present study, the geranylgeranyl chain of Rac1 plunges into a pocket defined by the immunoglobulin-like domain of RhoGDI (Figure 4a). The surface of this pocket mainly consists of conserved hydrophobic residues at van der Waals distances from the geranylgeranyl group. The insertion of the isoprenyl group perturbs the structure of RhoGDI as seen from comparison with the structure of the noncomplexed form of RhoGDI (*34*) (Figure 4b). First, the side chain of $Leu75_{GDI}$ flips to accommodate the geranylgeranyl group, which induces small changes in the position of $Ile114_{GDI}$ and a significant shift (4−5 Å) of $Phe181_{GDI}$. A movement of $Leu77_{GDI}$ is also observed. Globally, β-strands βH (residues 174−183) and βI (residues 190−199) move by 2.0 Å to overcome steric problems with the geranylgeranyl group. This shift involves $Tyr175_{GDI}$, $Ile177_{GDI}$ (βH) and $Trp194_{GDI}$, $Leu196_{GDI}$ (βI). Similar displacements of the β-strands have been described in the structure of Cdc42−RhoGDI (*19*).

Key Residues of Rac1 in the Interaction with RhoGDI. A number of Rac1 residues, $Thr35_{Rac}$, $Tyr64_{Rac}$, $Arg66_{Rac}$, $His103_{Rac}$, and $His104_{Rac}$ (Figure 5), are involved in hydrogen bonds with RhoGDI. The interaction between $Thr35_{Rac}$ and $Asp45_{GDI}$ is particularly important for inhibition of the GDP−GTP exchange. In the structure of RhoA(GDP) (*29*), the carbonyl group of $Thr37_{RhoA}$ coordinates to Mg^{2+}, and the side chain of $Thr37_{RhoA}$ is exposed to the solvent, whereas in Rac1(GMPPNP) (*30*) or RhoA(GTP-γ-S) (*31*) it is the hydroxyl of $Thr35_{Rac}$ (equivalent to $Thr37_{RhoA}$) that contacts the Mg^{2+}. In the Rac1−RhoGDI structure, Rac1 is in a GDP conformation with the carbonyl of $Thr35_{Rac}$ coordinating to Mg^{2+}. In the interaction with RhoGDI, GDP is strongly stabilized by a hydrogen bond between the hydroxyl group of $Thr35_{Rac}$ and $Asp45_{GDI}$. $Tyr64_{Rac}$ also interacts by its hydroxyl group with $Asp42_{GDI}$ and $Lys52_{GDI}$, which are located in the N-terminal α-helices of RhoGDI. Strong interaction of $Arg66_{Rac}$ with RhoGDI (Figure 6) occurs through hydrogen bonds with the carbonyl groups of $Pro30_{GDI}$ and $Ala31_{GDI}$ and the oxygen atoms of $Glu121_{GDI}$ and $Asp185_{GDI}$. $His103_{Rac}$ and $His104_{Rac}$, located at the C-terminal end of the α3 helix of Rac1, interact with $Asp184_{GDI}$ and $Tyr27_{GDI}$, respectively. As shown in Figure 6, $His103_{Rac}$ is localized in close proximity to the switch II region. Additionally to the interactions previously described, hydrophobic interactions between $Leu67_{Rac}$, $Leu70_{Rac}$, and residues $Ile38_{GDI}$, $Leu55_{GDI}$, $Leu56_{GDI}$, and $Ile122_{GDI}$ strengthen the stability of the Rac1−RhoGDI complex (Figure 6). Altogether, the interactions with RhoGDI of $Tyr64_{Rac}$, $Arg66_{Rac}$, $Leu67_{Rac}$, and $Leu70_{Rac}$ located in the switch II region of Rac1 maintain this region in a GTP-like conformation despite the fact that Rac1 binds a GDP molecule.

DISCUSSION

The overall structure of the Rac1−RhoGDI complex is globally similar to the recently reported structures of two related complexes, Cdc42−RhoGDI (*19*) and Rac2−LyGDI (*20*). The interest of the present study is that the Rac1-(GDP)−RhoGDI complex is able to activate the O_2^- generating NADPH oxidase, although its efficiency is somewhat lower than that of free Rac1(GTP). Comparison of the structures of different Rho proteins complexed with different forms of GDIs enabled us to localize a number of amino acids that appear to be critical in NADPH oxidase activation.

Specificity of Recognition between RhoGDI and RhoGTPases. The overall structures of small G proteins, described as the G domain, are very similar. Although RhoGTPases

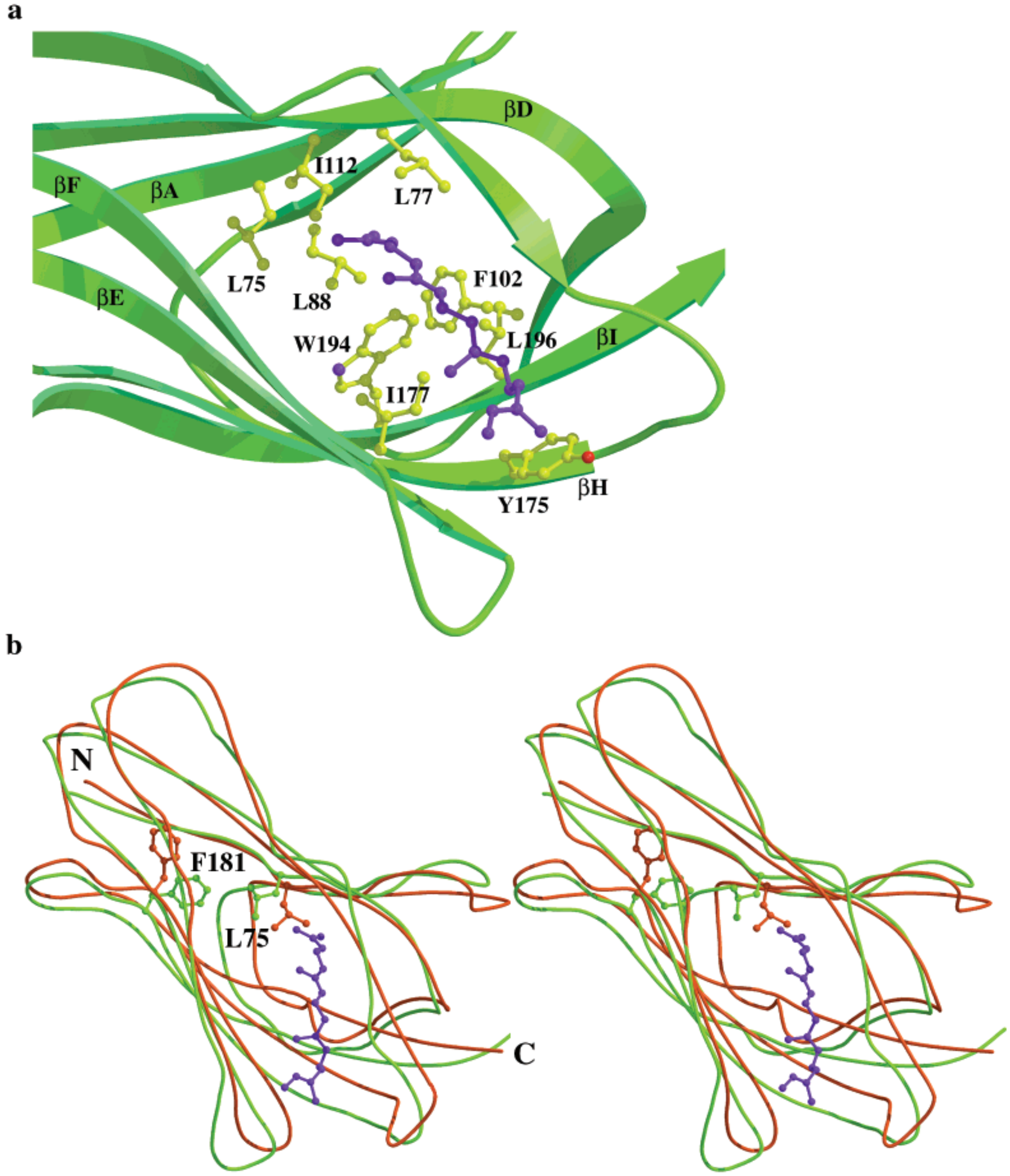

FIGURE 4: (a) Binding pocket of the geranylgeranyl tail. The hydrophobic residues of RhoGDI involved in interactions with the lipidic group (in dark blue) are labeled. (b) Structural changes in the core of RhoGDI induced by the geranylgeranyl tail of Rac1. The structure of the immunoglobulin core of RhoGDI within the Rac1−RhoGDI complex and the free RhoGDI (PDB accession code 1RHO) are represented in green and red, respectively. Side chain movements are illustrated for Leu75 and Phe181. The superimposition was done on the Cα atoms of residues 70−200 of RhoGDI.

```
               Switch I                    Switch II
          30        40        50        60
Rac1      TNAFPGEYIPTVFDNYSANVMVDGKPVNLGLWDTAGQEDYDRLR
Rac2      TNAFPGEYIPTVFDNYSANVMVDSKPVNLGLWDTAGQEDYDRLR
Cdc42     TNKFPSEYVPTVFDNYAVTVMIGGEPYTLGLFDTAGQEDYDRLR
RhoA      KDQFPEVYVPTVFENYVADIEVDGKQVELALWDTAGQEDYDRLR
RhoH      SETFPEAYKPTVYENTGVDVFMDGIQISLGLWDTAGNDAFRSIR
H-Ras     QNHFVDEYDPTIEDSYRKQVVIDGETCLLDILDTAGQEEYSAMR

          70        80        90        100        110
Rac1      PLSYPQTDVFLICFSLVSPASFENVRAKWYPEVR--HHCPNTPI
Rac2      PLSYPQTDVFLICFSLVSPASYENVRAKWFPEVR--HHCPSTPI
Cdc42     PLSYPQTDVFLVCFSVVSPSSFENVKEKWVPEIT--HHCPKTPF
RhoA      PLSYPDTDVILMCFSIDSPDSLENIPEKWTPEVK--HFCPNVPI
RhoH      PLSYQQADVVLMCYSVANHNSFLNLKNKWIGEIR--SNLPCTPV
H-Ras     DQYMRTGEGFLCVFAINNTKSFEDIH-QYREQIKRVKDSDDVPM
```

FIGURE 5: Sequence alignment between RhoGTPases and H-Ras. Residues involved in interaction with RhoGDI are boxed. Residues are numbered with respect to Rac1.

share 20% identity with Ras, they differ by the absence of interaction of Ras with RhoGDI. The specificity of recognition between RhoGDI and Rac1, and more widely the small G proteins of the Rho family, involves conserved residues in the two proteins. $Arg66_{Rac}$ and $His103_{Rac}$ are conserved residues among the members of the Rho family found to interact with RhoGDI (Figure 5). Interestingly, they are not present in RhoH that interacts very weakly with RhoGDI (*35*), and they are also absent in Ras. Therefore, the specificity of the interaction between RhoGDI and Rho-related GTPases appears to be largely provided by $Arg66_{Rac}$ and $His103_{Rac}$. This conclusion is confirmed by two-hybrid experiments showing that the nonprenylated Rac1 Cys189Gly is still able to interact with RhoGDI but that additional mutations Arg66Ser or His103Ala result in a loss of interaction with RhoGDI (*36*). It is interesting to note that the $Leu67_{Rac}$ and $Leu70_{Rac}$ residues which are conserved in the Rho family are replaced in Ras by Met and Gln, respectively, and that the interacting hydrophobic amino acids

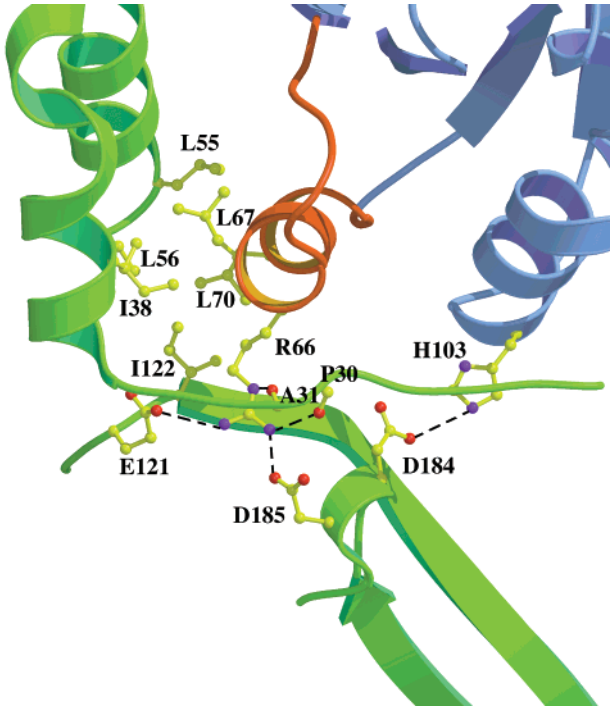

FIGURE 6: Structural determinants of the main interacting region of the Rac1−RhoGDI complex. The color codes are the same as in Figure 3. The hydrophobic interactions and the hydrogen bonds (dashed lines) made by $Arg66_{Rac}$ and $His103_{Rac}$ are represented.

in RhoGDI are conserved in the three isoforms of GDIs. The recognition of Rho proteins and not Ras proteins by RhoGDI cannot be explained by the different nature of the prenyl chain attached to the G protein, namely, a geranylgeranyl residue in the case of Rac1 and a farnesyl residue in that of Ras. In fact, *N*-acetylfarnesylcysteine methyl ester is able to bind to RhoGDI with a relatively high affinity (*37*). On the other hand, a few residues of the isoprene binding pocket of RhoGDI appear to modulate the affinity for RhoGTPases. This is the case for $Ile177_{GDI}$. LyGDI has a 15-fold lower affinity for prenylated Cdc42 (*13*, *38*). A factor that could explain this difference in affinity is the substitution of Ile177 in RhoGDI by Asn174 in LyGDI. This is consistent with the recently reported structure of Rac2−LyGDI (*20*), which does not show the geranylgeranyl group in the hydrophobic pocket of LyGDI despite a better resolution, while in the 2.6 Å structure of the Cdc42−RhoGDI complex, the geranylgeranyl group is detected in an omit electron density map. In this latter structure as well as in the structure presented here, the geranylgeranyl group is refined with high *B*-factors. Since almost all the changes due to the presence of the geranylgeranyl group described above are present in the Rac2−LyGDI complex, it is likely that the isoprenyl group was present in the pocket of LyGDI, but that its conformation, due to the absence of firm binding, was too disordered and therefore not visible in the electron density map.

In summary, a number of protein−protein interactions, in addition to the lipid−protein interaction via the geranylgeranyl group of Rac1, are involved in the specific recognition, by RhoGDI, of the RhoGTPases.

Inhibition of the GDP−GTP Exchange Reaction. Although small G proteins can release their bound GDP at low Mg^{2+} concentrations, this release in the cell is catalyzed by GEFs. $Thr35_{Rac}$ is a highly conserved residue in all GTP-binding proteins. It coordinates to Mg^{2+} and therefore contributes to the stabilization of the nucleotide. Analysis of interactions between Ras devoid of nucleotide and its specific GEF, Sos, suggests that, in this structure, the switch II region and to a lesser extent the switch I region of Ras might be essential for the binding of Ras to Sos (*39*). Biochemical data indicate that switch II is not as important as switch I for the interaction between Rho proteins and their respective GEFs (*40*). In addition, the Thr35Ala mutant of Cdc42 (or Thr37Ala for Rho) loses responsiveness to GEF, whereas the same mutation on Ras reduces its affinity by 3-fold (*41*). These results point to different modes of interaction between the various families of the small G proteins and their GEFs, with a predominant role of switch I in the Rho family. It has been recently reported that the GEF Tiam1 strongly interacts with both switch I and switch II of Rac1 (*42*). Thus, the Rac1−RhoGDI complex has to be dissociated to allow Rac1 to interact with its GEF.

Rac1−RhoGDI and the NADPH Oxidase. Rac is a key component of the O_2^- generating NADPH oxidase complex of phagocytes that is activated in response to microbial infection (*43*). The Rac1−RhoGDI heterodimer has been found to be an activating factor of the NADPH oxidase complex like free Rac(GTP) (*3*). The same observation holds for the activation of phospholipase Cβ2 by the Rac1−LyGDI heterodimer (*44*). $p67^{phox}$, one of the cytosolic factors of the NADPH oxidase complex, binds to Rac(GTP) and appears to be the effector protein of Rac(GTP) in oxidase activation (*45*). Structures of complexes involving Cdc42 and effector proteins that contain a CRIB motif like WASP or PAK have been recently reported (*46*, *47*). These interactions involve residues of Cdc42 that are mainly masked in the Cdc42−RhoGDI complex. In contrast to these structures, the structure of Rac1(GTP) associated with the N-terminal part of $p67^{phox}$ shows another mode of interaction of a small GTPase with its effector (*48*), which involves switch I residues as well as residues 159−162 of Rac1. Point mutations in the switch I region were previously shown to impair the binding of Rac1 to $p67^{phox}$ (*49*). In particular, $Ala27_{Rac}$ and $Gly30_{Rac}$ are not conserved in Cdc42. Substitution of Cdc42 residues in positions 27 and 30 by corresponding residues found in Rac1 renders Cdc42 competent for NADPH oxidase activation (*50*). In addition, the Rho-specific insert region (residues 122−137) is needed for full NADPH oxidase activation (*51*). The following residues of Rac1, 26−31 of switch I, 159−162, and these of the Rho-specific insert region are accessible in the Rac1−RhoGDI complex. Since free Rac1 has two interacting regions with $p67^{phox}$ (*48*), low-affinity binding of Rac(GDP) associated with RhoGDI to $p67^{phox}$ could occur. These features would explain why the Rac1−RhoGDI complex is competent for oxidase activation in an in vitro system, yet with a lower efficiency than Rac(GTP).

ACKNOWLEDGMENT

The authors thank Nicolas Nassar and Zigmunt Derewenda for providing the crystallographic coordinates of the Cdc42−RhoGDI complex and the RhoA−RhoGDI complex and Laurent Chantalat for helpful discussions.

REFERENCES

1. Hall, A. (1998) *Science 279*, 502−514.
2. Dehnardt, D. T. (1996) *Biochem. J. 318*, 729−747.

3. Abo, A., Pick, E., Hall, A., Potty, N., Teahan, C. G., and Segal, A. W. (1991) *Nature 353*, 668−670.
4. Geyer, A., and Wittinghofer, A. (1997) *Curr. Opin. Struct. Biol. 7*, 786−792.
5. Knaus, U. G., Heyworth, P. G., Kinsella, B. T., Curnutte, J. T., and Bokoch, G. M. (1992) *J. Biol. Chem. 267*, 23575−23582.
6. Haataja, L., Groffen, J., and Heisterkamp, N. (1997) *J. Biol. Chem. 272*, 20384−20388.
7. Bourmeyster, N., Stasia, M. J., Garin, J., Gagnon, J., Boquet, P., and Vignais, P. V. (1992) *Biochemistry 31*, 12863−12869.
8. Scherle, P., Behreus, T., and Staudt, L. M. (1993) *Proc. Natl. Acad. Sci. U.S.A. 90*, 7568−7572.
9. Lelias, J. M., Adra, C. N., Wulf, G. M., Guillemot, J. C., Khagad, M., Caput, D., and Lim, B. (1993) *Proc. Natl. Acad. Sci. U.S.A. 90*, 1479−1483.
10. Adra, C. N., Manor, D., Ko, J. L., Zhu, S., Horiuchi, T., Van Aelst, L., Cerione, R. A., and Lim, B. (1997) *Proc. Natl. Acad. Sci. U.S.A. 94*, 4279−4284.
11. Ohaga, N., Kikuchi, A., Ueda, T., Yamamoto, J., and Takai, Y. (1989*) Biochem. Biophys. Res. Commun. 163*, 1523−1533.
12. Hart, M. J., Maru, Y., Leonard, D., Witte, O. N., Evans, T., and Cerione, R. A. (1992) *Science 258*, 812−815.
13. Nomanbhoy, T. K., and Cerione, R. A. (1996) *J. Biol. Chem. 271*, 10004−10009.
14. Fauré, J., Vignais, P. V., and Dagher, M. C. (1999) *Eur. J. Biochem. 262*, 879−889.
15. Sasaki, T., and Takai, Y. (1998) *Biochem. Biophys. Res. Commun. 245*, 641−645.
16. Danley, D. E., Chuang, T. H., and Bokoch, G. M. (1996) *J. Immunol. 157*, 500−503.
17. Na, S., Chuang, T. H., Cunnigham, A., Turi, T. G., Hanke, J. H., Bokoch, G. M., and Danley, D. E. (1996) *J. Biol. Chem. 271*, 11209−11213.
18. Krieser, R. J., and Eastman, A. (1999) *Cell Death Differ. 6*, 412−419.
19. Hoffman, G. R., Nassar, N., and Cerione, R. A. (2000) *Cell 100*, 345−356.
20. Scheffzek, K., Stephan, I., Jensen, O. N., Illenberger, D., and Gierschik, P. (2000) *Nat. Struct. Biol. 7*, 122−126.
21. Grizot, S., Grandvaux, N., Fieschi, F., Fauré, J., Massenet, C., Andrieu, J.-P., Fuchs, A., Vignais, P. V., Timmins, P. A., Dagher, M.-C., and Pebay-Peyroula, E. (2001) *Biochemistry 40*, 3127−3133.
22. Otwinowski, Z., and Minor, W. (1997) *Methods Enzymol. 276*, 307−326.
23. Navaza, J. (1994) *Acta Crystallogr. A50*, 157−163.
24. Longenecker, K., Read, P., Derewenda, U., Dauter, Z., Liu, X., Garrard, S., Walker, L., Somlyo, A. V., Nakamoto, R. K., Somlyo, A. P., and Derewenda, Z. S. (1999) *Acta Crystallogr. D55*, 1503−1515.
25. Jones, T. A., Zou, J. Y., Cowan, S. W., and Kjeldgaard, M. (1991) *Acta Crystallogr. A47*, 110−119.
26. Brünger, A. T., Adams, P. D., Clore, G. M., Gros, P., Grosse-Kuntsleve, R. W., Tiang, J. S., Kuszewski, J., Nilges, M., Pannu, N. S., and Read, R. J. (1998) *Acta Crystallogr. D54*, 905−921.
27. Kraulis, P. J. (1991) *J. Appl. Crystallogr. 24*, 946−950.
28. Merritt, E. A., and Murphy, M. E. P. (1994) *Acta Crystallogr. D50*, 869−873.
29. Wei, Y., Zhang, Y., Derewenda, U., Liu, X., Minor, W., Nakamoto, R. K., Smolyo, A. V., Somlyo, A. P., and Derewenda, Z. S. (1997) *Nat. Struct. Biol. 4*, 699−703.
30. Hirschberg, M., Stockley, R. W., Dodson, G., and Webb, M. R. (1997) *Nat. Struct. Biol. 4*, 147−152.
31. Ihara, K., Muraguchi, S., Kato, H., Shimizu, T., Shirakawa, H., Kuroda, S., Kaibuchi, K., and Hakoshima, T. (1998) *J. Biol. Chem. 273*, 9656−9666.
32. Wu, W. J., Leonard, D. A., Cerione, R. A., and Manor, D. (1997) *J. Biol. Chem. 272*, 26153−26158.
33. Gosser, Y. Q., Nomanbhoy, T. K., Aghazadeh, B., Manor, D., Combs, C., Cerione, R. A., and Rosen, M. K. (1997) *Nature 387*, 814−819.
34. Keep, N. H., Barnes, M., Barsukov, I., Badii, R., Liam, L. Y., Segal, A. W., Moody, P. C., and Roberts, G. C. (1997) *Structure 5*, 623−633.
35. Fauré, J., and Dagher, M.-C. (2001) *Biochimie 83*, 409−414.
36. Di-Poï, N., Fauré, J., Grizot, S., Molnár, G., Pick, E., and Dagher, M.-C. (2001) *Biochemistry 40*, 10014−10022.
37. Mondal, M. S., Wang, Z., Seeds, A. M., and Rando, R. R. (2000) *Biochemistry 39*, 406−412.
38. Platko, J. V., Leonard, D. A., Adra, C. N., Shaw, R. J., Cerione, R. A., and Lim, B. (1995) *Proc. Natl. Acad. Sci. U.S.A. 92*, 2974−2978.
39. Boriack-Sjodin, P. A., Margarit, S. M., Bar-Sagi, D., and Kuriyan, J. (1998) *Nature 394*, 337−343.
40. Li, R., and Zheng, Y. (1997) *J. Biol. Chem. 272*, 4671−4679.
41. Mitsou, M. Y., Jacquet, E., Poullet, P., Rensland, H., Gideon, P., Schlichting, I., Wittinghofer, A., and Parmeggiani, A. (1992) *EMBO J. 11*, 2391−2397.
42. Worthylake, D. K., Rossman, K. L., and Sondek, J. (2000) *Nature 408*, 682−688.
43. Babior, B. M. (1999) *Blood 93*, 1464−1476.
44. Illenberger, D., Schwald, F., Pimmer, D., Binder, W., Maier, G., Dietrich, A., and Gierschik, P. (1998) *EMBO J. 17*, 6241−6249.
45. Diekmann, D., Abo, A., Johnston, C., Segal, A. W., and Hall, A. (1994) *Science 265*, 531−533.
46. Abdul-Manan, N., Aghazadeh, B., Liu, G. A., Majumdar, A., Ouerfelli, O., Siminovitch, K. A., and Rosen, M. K. (1999) *Nature 399*, 379−383.
47. Morreale, A., Venkatesan, M., Mott, H. R., Owen, D., Nietlispach, D., Lowe, P. N., and Laue, E. D. (2000) *Nat. Struct. Biol. 7*, 384−388.
48. Lapouge, K., Smith, S. J., Walker, P. A., Gamblin, S. J., Smerdon, S. J., and Rittinger, K. (2000) *Mol. Cell 6*, 899−907.
49. Nisimoto, Y., Freeman, J. L., Motalebi, S. A., Hirschberg, M., and Lambeth, J. D. (1997) *J. Biol. Chem. 272*, 18834−18841.
50. Kwong, C. H., Adams, A. G., and Leto, T. L. (1995) *J. Biol. Chem. 270*, 19868−19872.
51. Freeman, J. L., Abo, A., and Lambeth, J. D. (1996) *J. Biol. Chem. 271*, 19794−19801.

BI010288K